Supporting information:

Discrete Ag_6L_6 Coordination Nanotubular Structures Based on a T-shaped Pyridyl Diphosphine

Xiaobing Wang,[a] Jing Huang,[a] Shenglin Xiang,[a] Yu Liu,[a] Jianyong Zhang,*[a] Andreas Eichhöfer,[b] Dieter Fenske,[b] Shi Bai[c] and Cheng-Yong Su*[a]

[a] *KLGHEI of Environmental and Energy Chemistry, MOE Laboratory of Bioinorganic and Synthetic Chemistry, State Key Laboratory of Optoelectronic Materials and Technologies, School of Chemistry and Chemical Engineering, Sun Yat-Sen University, Guangzhou 510275, China. E-mail: zhjyong@mail.sysu.edu.cn*

[b] *Forschungszentrum Karlsruhe, Institut für Nanotechnologie, Postfach 3640, 76021 Karlsruhe, Germany*

[c] *Department of Chemistry and Biochemistry, University of Delaware, Newark, DE 19716-2502, USA*

Experimental section

General method. All starting materials and solvents were obtained from commercial sources and used without further purification unless otherwise stated. 4-(3,5-difluotophenyl)-pyridine was synthesised following the reported method.[1] ^{1}H and $^{31}P\{^{1}H\}$ NMR spectra were recorded on a Mercury Plus 300 MHz spectrometer at ca. 300 K at the operating frequencies of 300.0 and 121.5 MHz, respectively. 2D NMR spectra were recorded on a Bluker AVANCE AV 400 Superconducting Fourier Transform Nuclear Magnetic Resonance Spectrometry. ESI-TOF mass spectra were recorded on a Time of Flight (TOF) mass spectrometer (Bruker Daltonics, MicroTOF-QII) equipped with an electrospray ion source (off axis sprayer) in the positive-ion mode with MeOH as mobile phase by dissolving a crystalline sample in

CH_3NO_2. Assignment of major ions was aided by a comparison of the experimental and calculated isotope distribution patterns. FT-IR spectra were recorded on a Nicolet Avatrar 330 FT-IR spectrometer with KBr pellets.

Synthesis of 4-(3,5-bis(diphenylphosphino)phenyl)pyridine (L). The reaction was performed under pure dry nitrogen using standard Schlenk techniques. THF was distilled over K under nitrogen prior to use. To 4-(3,5-difluotophenyl)-pyridine (0.50 g, 2.61 mmol) in THF (10 ml) was added dropwise $KPPh_2$ (10.5 ml, 0.5 mol/l, 5.25 mmol) with stirring. The reaction mixture was brought to reflux for 5 hours. THF was removed under reduced pressure and methanol (5 ml) was added to obtain a white precipitate. The white solid was collected by filtration and washed with Et_2O (3 × 5 ml) (0.78 g, yield 57%). ^{1}H NMR (300 MHz, d_6-DMSO): δ = 8.54 (d, 2H, $^3J_{H-H}$ = 4.8 Hz), 7.66 (d, 2H, $^3J_{H-P}$ = 7.8 Hz), 7.51 (d, 2H, $^3J_{H-H}$ = 4.8 Hz), δ = 7.35 (m, 12 H), 7.18 (m, 8H), 6.98 (t, 1H, $^3J_{H-P}$ = 5.7 Hz); ^{31}P NMR (121 MHz, d_6-DMSO): δ = –6.46.

*($Ag_6L_6 \supset 2SbF_6$)·(SbF_6)$_4$ (**Ag_6L_6–SbF_6**).* A buffer layer of $CHCl_3$–CH_3OH (v:v = 1:1, 2 ml) was carefully layered over a solution of L (10.5 mg, 0.02 mmol) in $CHCl_3$ (2 ml). Then a solution of $AgSbF_6$ (6.9 mg, 0.02 mmol) in CH_3OH (2 ml) was layered over the buffer layer. After ca. 3 days, colourless block crystals were obtained (5.3 mg, yield 30%). Elemental analysis for $C_{210}H_{162}Ag_6F_{36}N_6P_{12}Sb_6 \cdot CHCl_3$: found (calc.) C 47.46 (47.70), H 3.22 (3.07), N 1.53 (1.58)%. Fragment assignment [*m/z*, relative intensity(%)]: $[L_2Ag_2SbF_6]^+$ (1499.0, 90%), $[L_3Ag_3SbF_6]^{2+}$ (1064.6, 100%), $L_6Ag_6(SbF_6)_4^{2+}$, (2366.0, 7%), plus other unidentified ions. IR (KBr, cm^{-1}): ν = 3422 br, 3055s, 1816m, 1607s, 1544s, 1480s, 1436m, 1404s, 1328s, 1311s, 1256s, 1222s, 1185s, 1160s, 1124s, 1098s, 1066s, 1026s, 999s, 827s, 797s, 745m, 694w, 659w (SbF_6^-), 598s, 557s, 507s, 463s.

*[$LAg_2(CF_3CO_2)_2(H_2O)(Et_2O)]_n$ (**Ag-TFA**).* A solution of L (2.6 mg, 0.005 mmol) in $CHCl_3$ (1 mL) was added to a stirred solution of $AgCF_3CO_2$ (1.7 mg, 0.0075 mmol) in CH_3CN (1mL). The solution mixture was stirred for 10 min under dark conditions.

Et_2O vapour was diffused into the solution mixture. Colourless block crystals were obtained after 1-2 days (1.2 mg, yield 30%). Elemental analysis for $C_{43}H_{39}Ag_2NO_6P_2F_6{\cdot}H_2O$ ($LAg_2(TFA)_2(H_2O){\cdot}H_2O$): found (calc.) C 48.35 (48.02), H 3.90 (3.84), N 1.27 (1.30)%. IR (KBr, cm^{-1}): ν = 3435s, 3055s, 1668s (νCOO), 1434s, 1200s, 1133s (νCO, νC-F), 694s, 597s.

*$[LAg_2(OTs)_2(CHCl_3)]_n$ (**Ag-OTs**).* A solution of L (2.6 mg, 0.005 mmol) in $CHCl_3$ (1 mL) was added to a stirred solution of AgOTs (1.2 mg, 0.0075 mmol) in CH_3CN (1 mL). The solution mixture was stirred for 10 min under dark conditions. Et_2O vapour was diffused into the solution mixture. Colourless block crystals were obtained after 1-2 days (1.8 mg, yield 40%). Elemental analysis for $C_{49}H_{39}Ag_2NO_5P_2S_2{\cdot}H_2O$ ($Ag_2L(OTs)_2{\cdot}H_2O$): found (calc.) C 53.83 (53.52), H 3.84 (3.94), N 1.41 (1.27)%. IR (KBr, cm^{-1}): ν = 3434s, 3053s, 1606s, 1435s, 1192s (S=O), 692s, 571s.

X-ray crystallographic analyses. The X-ray diffraction data were collected on an Oxford Germini S Ultra diffractometer with graphite monochromated Cu Kα radiation (λ = 1.54178 Å) for **Ag_6L_6-SbF_6** and **Ag-OTs** while Mo Kα radiation (λ = 0.71073 Å) for **Ag-TFA** at 150 K. All the structures were refined anisotropically by the full-matrix least-squares method on F^2 for no-hydrogen atoms using SHELXL-97 except those disordered ones.[2] The hydrogen atoms were placed in calculated positions and refined using a riding model. For **Ag_6L_6-SbF_6**, due to a large number of disordered solvent molecules outside the tubular cavity, the structure was treated by the program SQUEEZE in PLATON to remove all the solvents.[3] The remaining significant residual density is close to Sb atoms and left as it is. All the phenyl and pyridyl rings were constrained to ideal hexagons with restraints described in detail in the CIF file. Disorder of the phenyl rings was only partly treated due to poor crystal quality but large molecule. One of the CF_3 groups in **Ag-TFA** was disordered and treated in fractional and constrained model (see details in the CIF file). Details of the crystal parameters, data collection, and refinements are summarised in Table S1.

CCDC 802912–802914 contain the supplementary crystallographic data.

(1) X. B. Wang, L. S. He, Y. He, J. Y. Zhang and C. Y. Su, *Inorg. Chim. Acta,* 2009, **362**, 3513–3518.

(2) G. M. Sheldrick, *SHELXL 97, Program for Crystal Structure Solution and Refinement*, Göttingen University, Germany, 1997.

(3) A. L. Spek, *Acta Crystallogr. Sect. A* 1990, **46**, C34.

Table S1. Crystallographic data for **Ag_6L_6-SbF_6**, **Ag-TFA** and **Ag-OTs**.

	Ag_6L_6-SbF_6	**Ag-TFA**	**Ag-OTs**
Formula	$C_{210}H_{162}Ag_6F_{36}N_6P_{12}Sb_6$	$C_{43}H_{39}Ag_2F_6NO_6P_2$	$C_{50}H_{42}Ag_2Cl_3NO_6P_2S_2$
M_w	5202.82	1057.43	1201.00
T (K)	150(2) K	150(2) K	150(2) K
crystal system	Monoclinic	Monoclinic	Monoclinic
space group	P2(1)/n	P2(1)/c	P2(1)/n
a/Å	18.4879(6)	11.3131(6)	10.6348(5)
b/Å	34.8299(11)	21.5140(9)	24.7251(11)
c/Å	20.2362(10)	18.1697(8)	19.4535(10)
α/º	90	90	90
β/º	102.860(4)	90.950(5)	103.775(5)
γ/º	90	90	90
V/Å^3	12703.9(9)	4421.7(4)	4968.1(4)
Z	2	4	4
D_{calcd}/g cm^{-1}	1.360	1.588	1.606
μ/mm^{-1}	8.898	1.030	9.608
F(0 0 0)	5112	2120	2416
θ range/º	2.57 to 61.61	2.61 to 26.00	2.94 to 62.60
no. reflns. collected	93050	23491	13858
no. inde. reflns.	10309	8612	7505
R_{int}	0.0853	0.0629	0.0767
data/restr./para.	10309/2035/1125	8612/90/513	7505/6/595
R_1 [$I > 2\sigma(I)$]	0.1116	0.0766	0.0550
wR_2 [$I > 2\sigma(I)$]	0.2544	0.2011	0.1651
R_1 (all data)	0.1550	0.1311	0.0831
wR_2 (all data)	0.2789	0.2182	0.1789
GOF	1.022	1.033	1.089

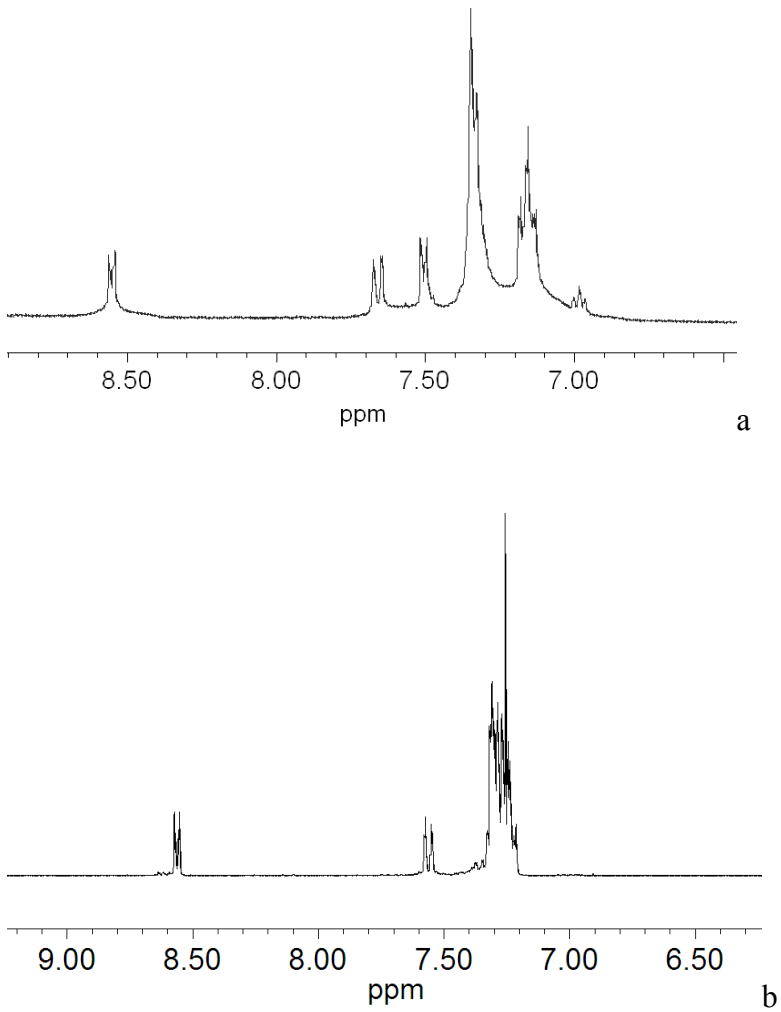

Figure S1. ^{1}H NMR of L in DMSO (a) and $CDCl_3$ (b), 300 MHz, 300 K.

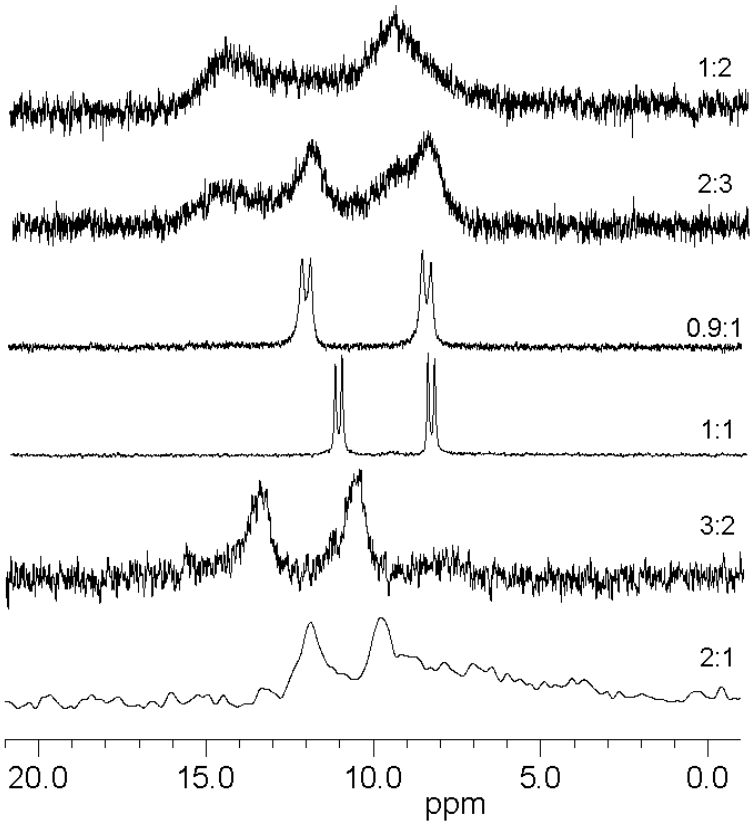

Figure S2. $^{31}P\{^{1}H\}$ NMR (121.5 MHz) spectra for different L/$AgBF_4$ ratios recorded at 300 K (1:2, 2:3 and 0.9:1 in $CDCl_3$–MeCN (v:v = 3:1); 1:1, 1.5:1 and 2:1 in $CDCl_3$-$MeNO_2$ (v:v = 3:1). Different solvent systems were used due to the solubility).

Because the solvents used for NMR are different, the coupling constants are different between in $CDCl_3$-$MeNO_2$ ($^{1}J(^{109}Ag\text{-}^{31}P)$ = 311 Hz) and in $CDCl_3$-MeCN ($^{1}J(^{109}Ag\text{-}^{31}P)$ = 407 Hz). However, the coupling constants are similar in one solvent system ($CDCl_3$-$MeNO_2$ or $CDCl_3$-MeCN) (see also below). The coupling constants are smaller in $CDCl_3$-$MeNO_2$ or CD_2Cl_2-$MeNO_2$ than those in $CDCl_3$-MeCN.

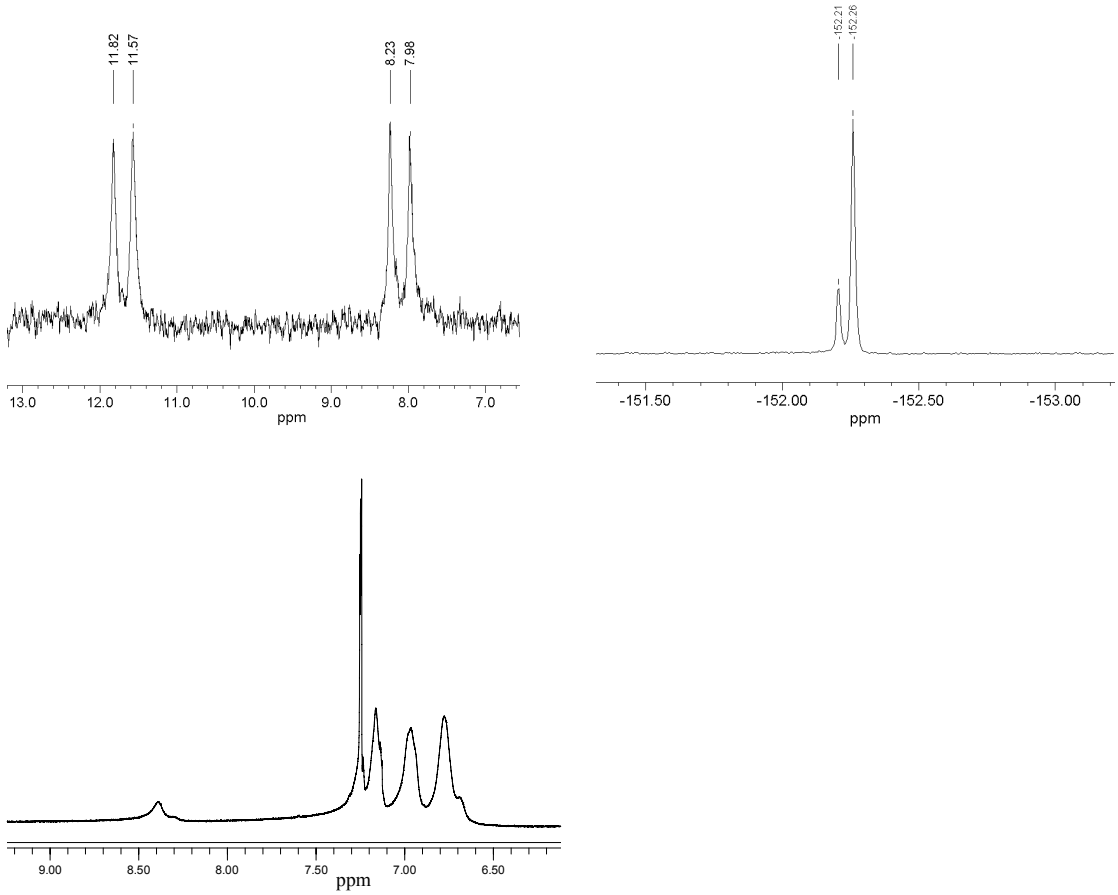

Figure S3. $^{31}P\{^{1}H\}$ NMR (121.5 MHz), ^{19}F NMR (282.3 MHz) and ^{1}H NMR (300 MHz) for L/$AgBF_4$ = 1:1 in $CDCl_3/CD_3CN$ (v:v = 2:1) at 300 K.

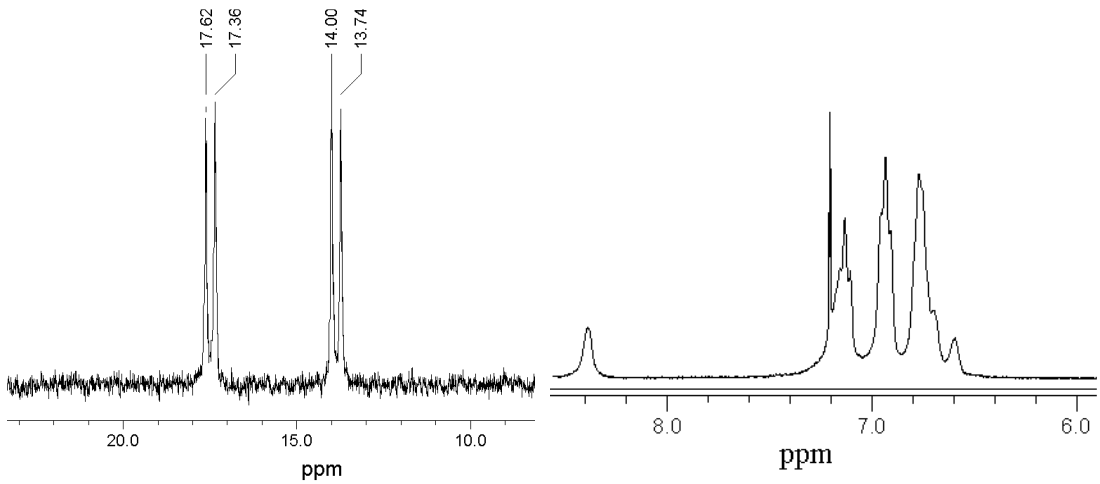

Figure S4. $^{31}P\{^{1}H\}$ NMR (121.5 MHz) and ^{1}H NMR (300 MHz) for L/$AgClO_4$ = 1:1 in $CDCl_3/CD_3CN$ (2:1) at 300 K.

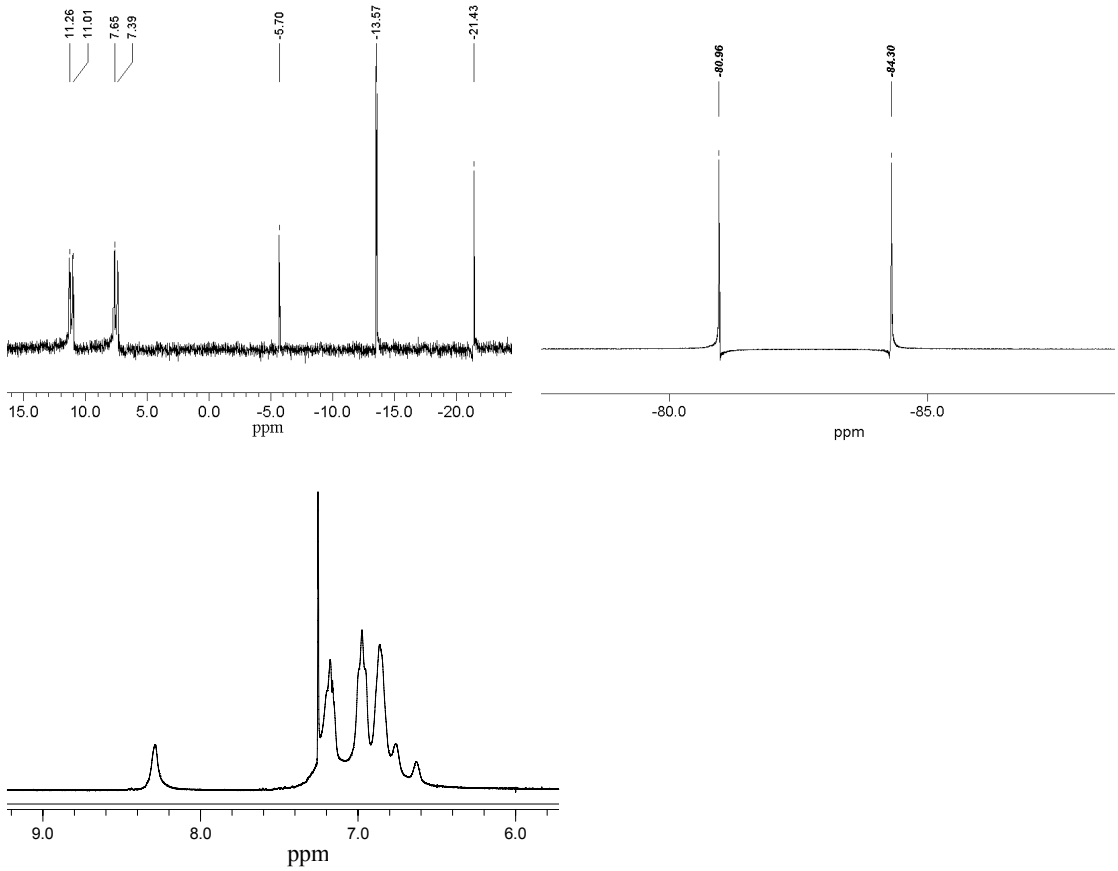

Figure S5. $^{31}P\{^{1}H\}$ NMR (121.5 MHz), ^{19}F NMR (282.3 MHz) and ^{1}H NMR (300 MHz) for L/$AgPF_6$ = 1:1 in $CDCl_3/CD_3CN$ (2:1) at 300 K.

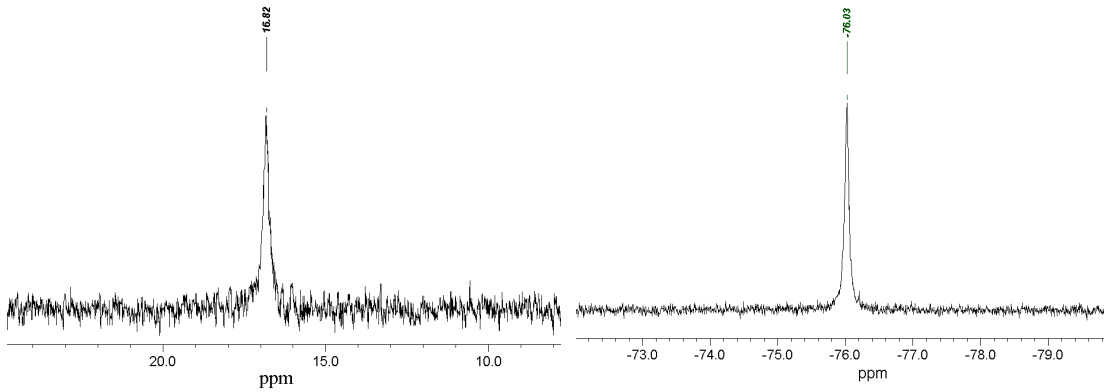

Figure S6. $^{31}P\{^{1}H\}$ NMR (121.5 MHz) and ^{19}F NMR (282.3 MHz) for L:AgTFA = 1:1 in $CDCl_3/CH_3CN$ (2:1) at 300 K.

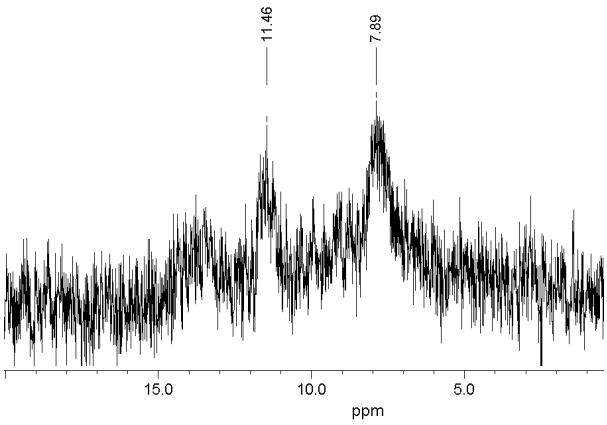

Figure S7. $^{31}P\{^{1}H\}$ NMR (121.5 MHz) for L:AgOTs = 1:1 in $CDCl_3/CH_3CN$ (2:1) at 300 K.

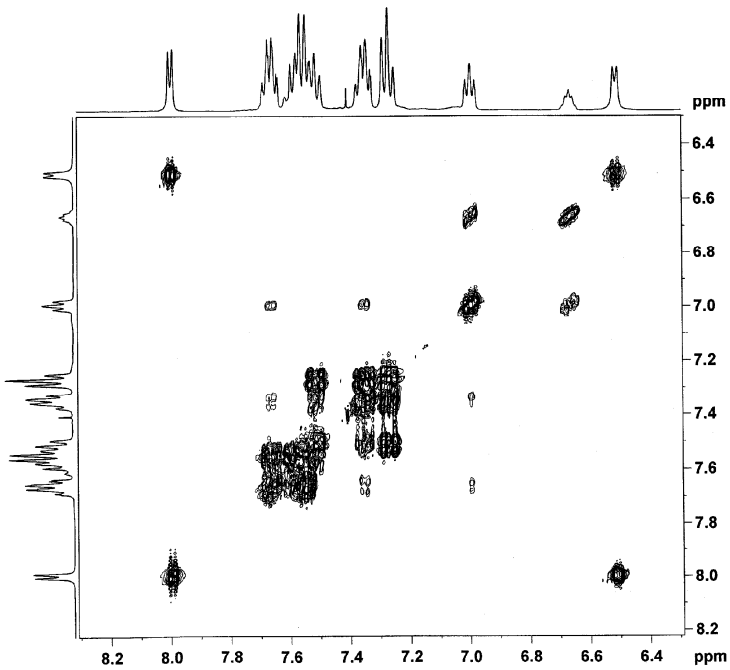

Figure S8. $^{1}H–^{1}H$ COSY spectrum of $\mathbf{Ag_6L_6–SbF_6}$ in CD_2Cl_2-CD_3NO_2 (v:v = 3:1) recorded at 300K, 400 MHz.

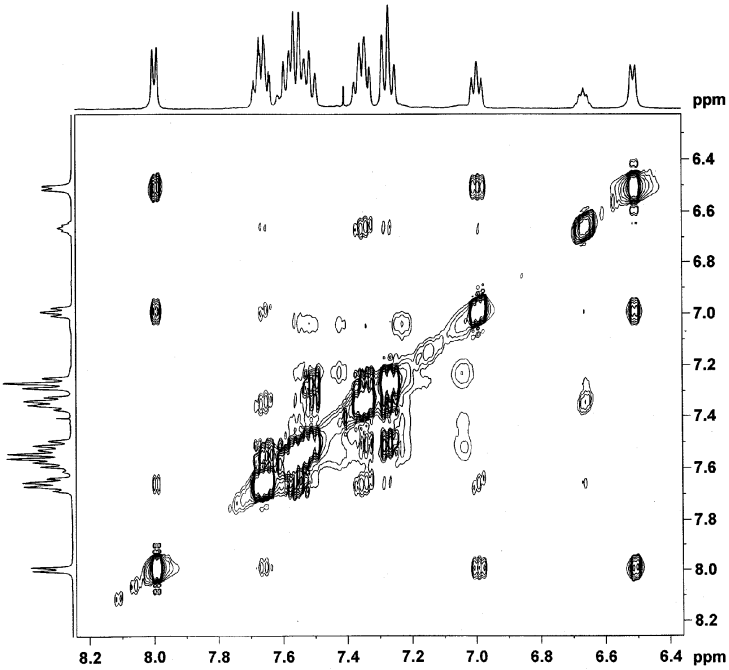

Figure S9. ^{1}H–^{1}H NOESY spectrum of **Ag_6L_6–SbF_6** in CD_2Cl_2-CD_3NO_2 (v:v = 3:1) recorded at 300K, 400 MHz.

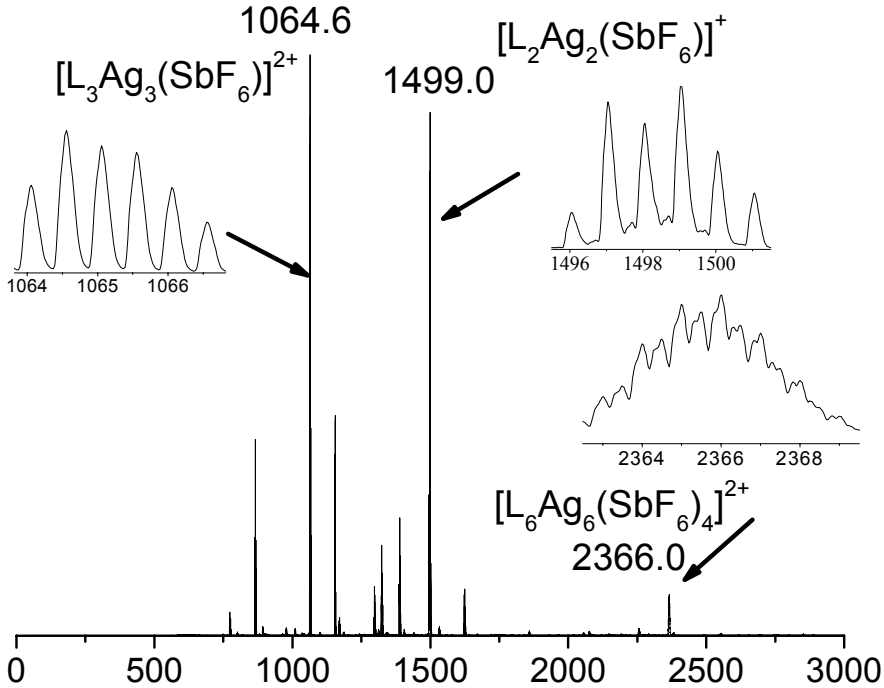

Figure S10. ESI-TOF mass spectrum of **Ag_6L_6-SbF_6** in nitromethane. The insets show assigned signals.

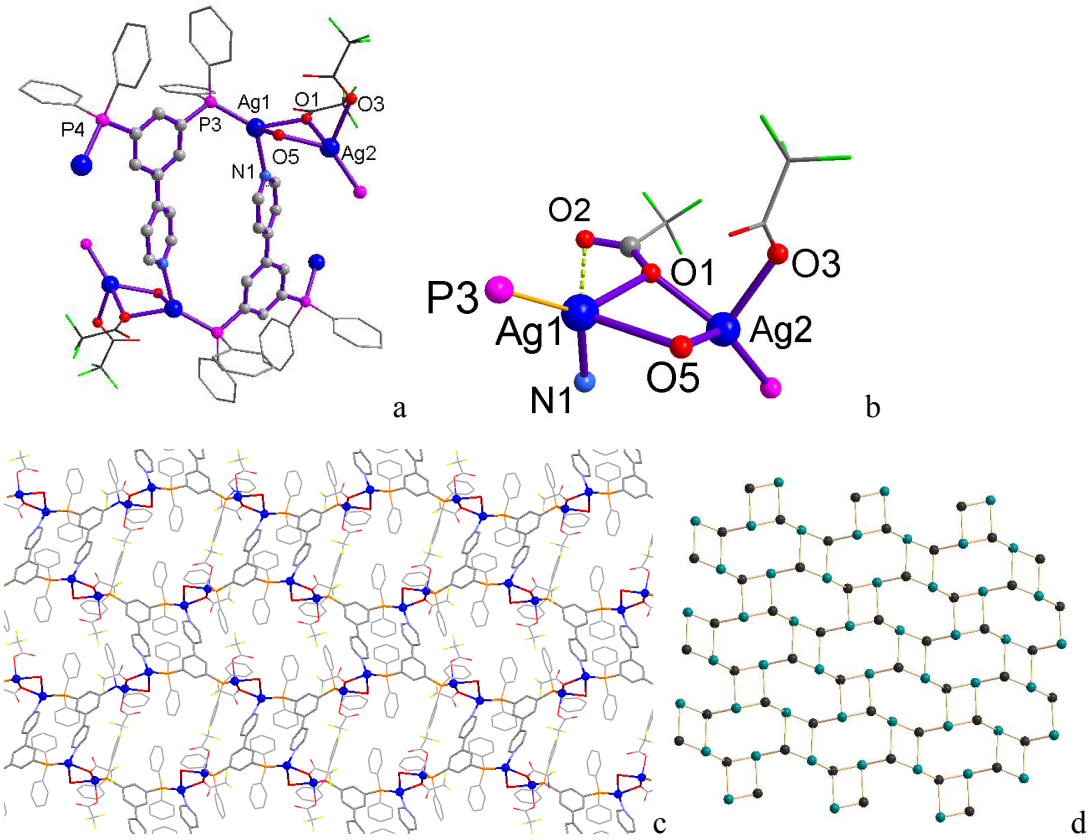

Figure S11. a, b) The coordination geometry around the Ag^+ ions, c) part of the 2D layer with Et_2O omitted for clarity; d) $(4,8^2)$ topology for **Ag-TFA**.

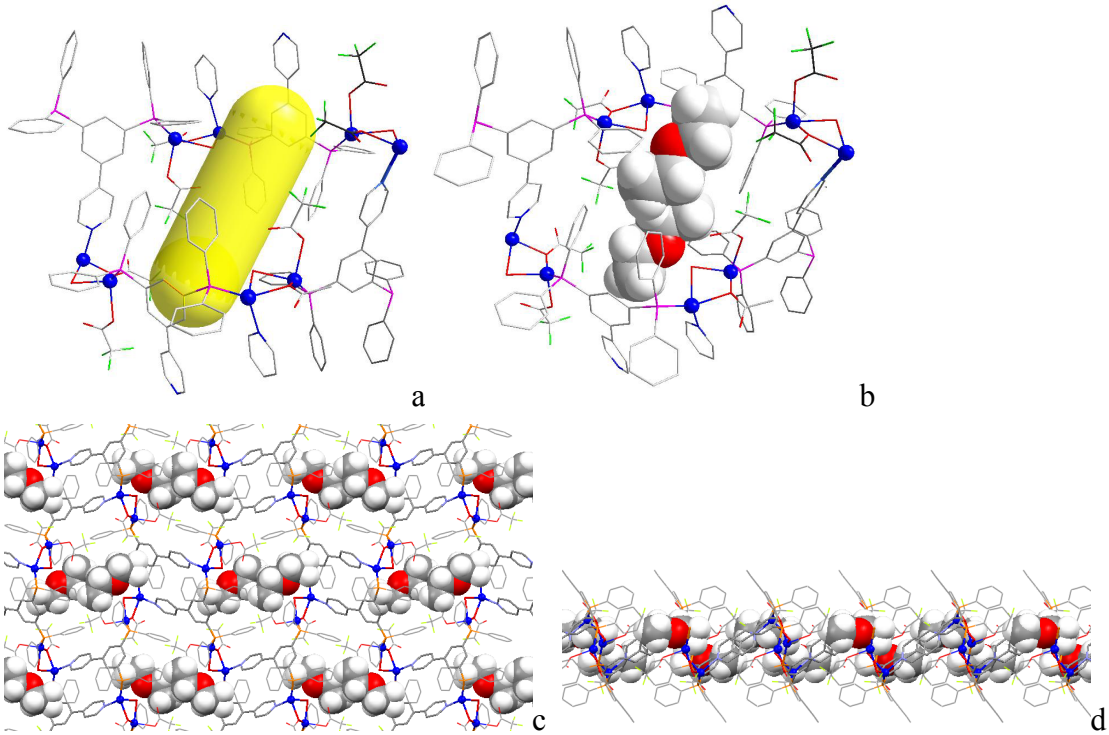

Figure S12. a) Cavity and b) a pair of Et_2O molecules located within the 2D layer, and views of a single layer along *a*-axis (c) and *b*-axis (d) for **Ag-TFA**.

There are two types of macrocyclic rings consisting of the 2D layers of **Ag-TFA**⊃Et_2O. The first type is an 18-membered ring formed by Ag_2L_2, and the second one is a 38–membered ring formed by Ag_4L_4. The 2D layers are stacked in an AAA fashion without interpenetration. The distance of the neighbouring layers is 21.51 Å (*b*). The Et_2O molecules are located within the layers. A pair of Et_2O solvent molecules is within each 38-membered ring, and each Et_2O molecule interact with the coordinated water molecule via O-H···O hydrogen bonding (O···O 2.761(12) Å). Opposite Ag···Ag distances are 11.4664(11) and 18.3726(12) Å within the 38-membered ring. The potential solvent-accessible occupancy volume is 15.9% calculated using PLATON (total potential solvent area volume 703.1 $Å^3$ per unit cell volume 4421.7 $Å^3$).

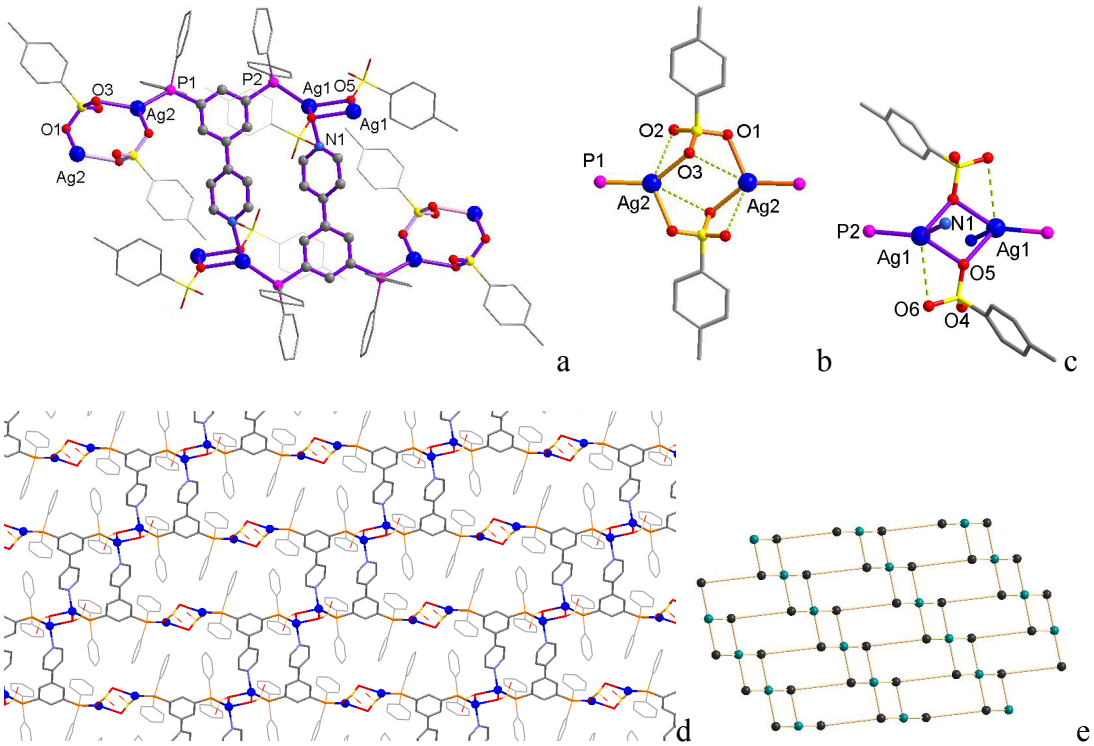

Figure S13. a, b, c) The coordination geometry around the Ag^+ ions, d) part of the 2D layer with $CHCl_3$ omitted for clarity, and e) $(4^2 6^2 8^2)(6^2,4)$ topology for **Ag-OTs**.

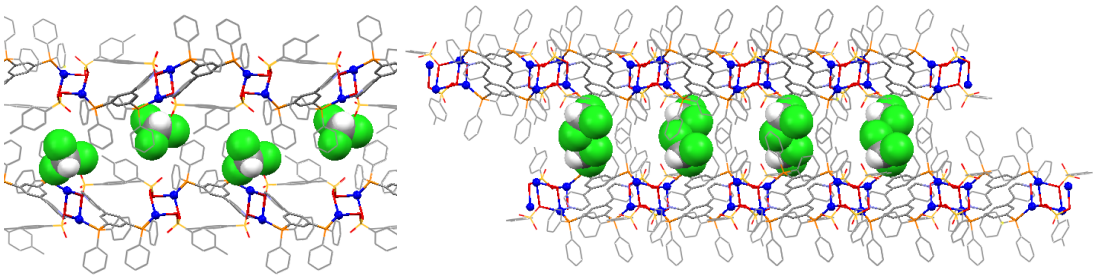

Figure S14. a) View along *a*-axis, and b) parallel stacking of 2D layers encapsulating solvated $CHCl_3$ molecules for **Ag-OTs**.

The 2D layers of **Ag-OTs**⊃Et_2O are consisted of two types of macrocyclic rings. The first type is an 18-membered ring formed by Ag_2L_2, and the second one is a 38–membered ring formed by Ag_4L_4. No solvent is located within the 2D layers. The 2D layers are stacked in an ABAB offset fashion without interpenetration. The distance of the neighbouring layers is 12.36 Å (*b*/2). There are cavities between the 2D layers formed by the phenyl rings of PPh_2 groups and the tolyl groups of the OTs^- anion. The $CHCl_3$ molecules are encapsulated in the cavities. The potential occupancy volume is 13.5% calculated using PLATON (total potential solvent area volume 672.4 $Å^3$ per unit cell volume 4968.1 $Å^3$).

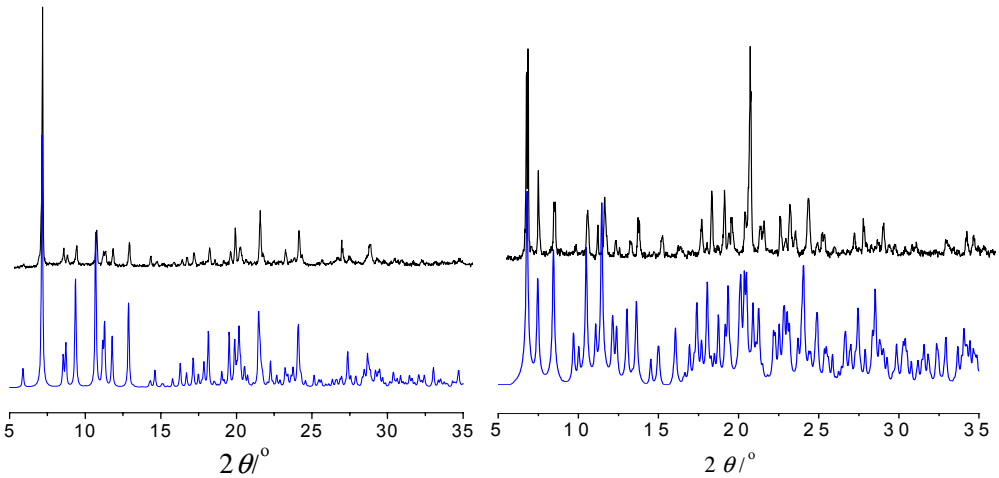

Figure S15. Power XRD patterns of **Ag-TFA** (left) and **Ag-OTs** (right) for the as-synthesised sample (top) and the simulated (bottom).

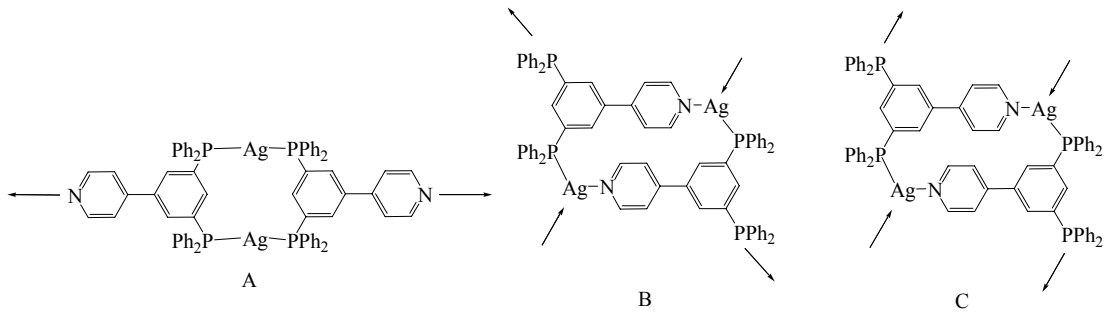

Scheme S1. Three possible dimeric synthons formed by L and Ag^+ according to the orientations of the lone pairs for *meta*-diphosphine groups: convergent conformation (A), alternate conformation (B), divergent conformation (C).

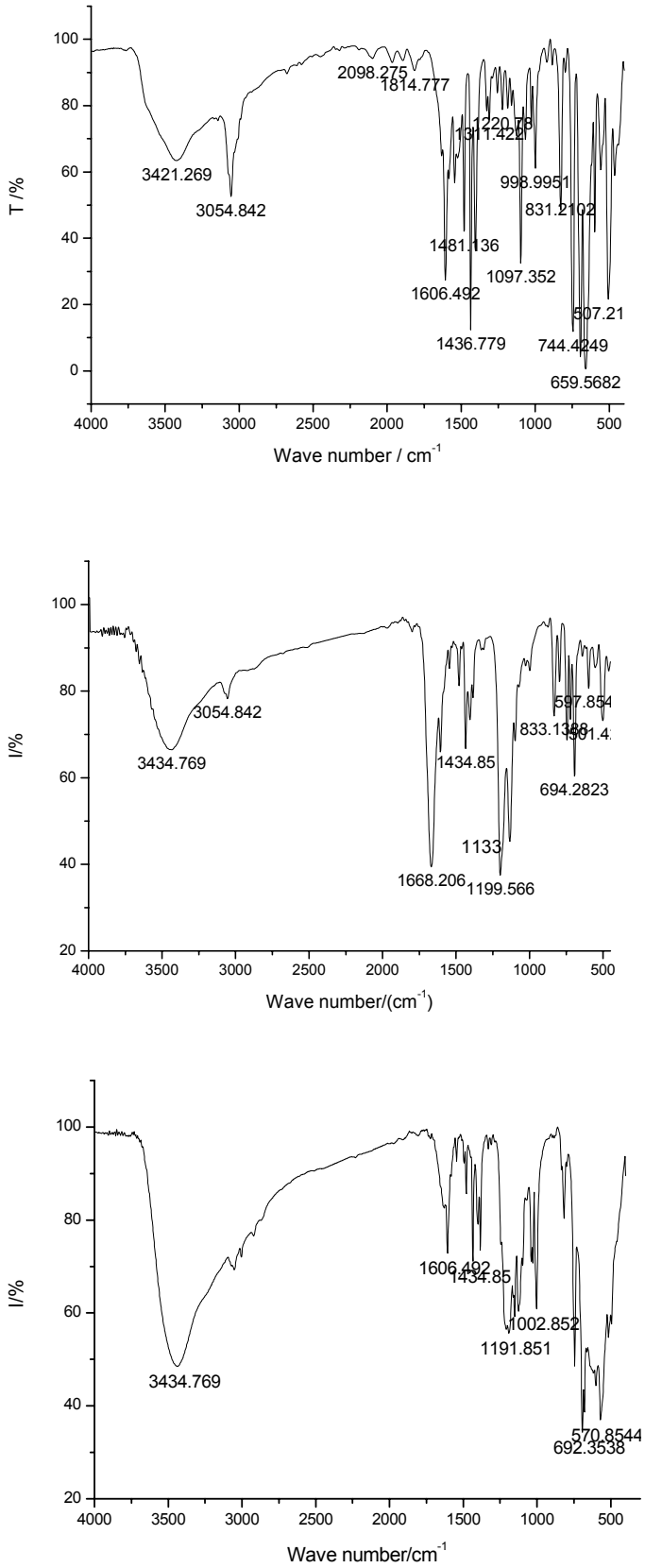

Figure S16. FT-IR spectra (KBr) of **Ag_6L_6-SbF_6**, **Ag-TFA** and **Ag-OTs**.